Journal of Korean Association of Crystal Growth
Vol. 6, No. 2 (1996) 141-154

Background impurity incorporation in the growth of InP by hydride vapor phase epitaxy technique

Chinho Park
School of Chemical Engineering and Technology, Yeungnam University, Kyungsan 712-749, Korea

Hydride 기상증착법을 이용한 InP 성장에서의 배경 불순물 도입에 관한 연구

박진호
영남대학교 화학공학 및 공업화학부, 경산, 712-749

Abstract Intrinsic layers of homoepitaxial InP grown by the hydride vapor phase epitaxy (VPE) technique were investigated by Fourier-transform photoluminescence (FTPL) and variable temperature Hall measurements. The effect of process variables (*i.e.*, source zone temperature and inlet mole fractions of HCl and PH_3) on the background impurity levels was investigated. The background carrier concentration was found to decrease with decreasing source zone temperature and increasing HCl, but was relatively independent of PH_3 for the range of mole fraction studied. The presence of background donors and acceptors was clearly verified in the FTPL spectra, and the major impurities were tentatively identified as Si donors and Zn acceptors as well as some unidentified acceptors.

요　　약 Hydride 기상증착법으로 성장시킨 InP 에피층들을 FTPL 분광법과 변온 Hall 측정법으로 조사하였다. 원료 공급 지역의 온도, 주입되는 HCl과 PH_3의 몰분율 등 공정변수가 배경 불순물의 주입에 미치는 영향을 조사한 결과, 배경 전하 농도는 원료 공급지역의 온도가 감소할수록 감소하고 HCl의 주입량이 증가할수록 감소하나 PH_3의 주입량에는 연구된 몰분율 범위 내에서 상대적으로 무관함을 알 수 있었다. 또한 FTPL spectrum 분석 결과 에피층 내부에 배경 donor들과 acceptor들이 존재함을 알 수 있었고 특히, Si donor들, Zn acceptor들, 확인되지 않은 acceptor들이 주된 불순물로 존재함을 알 수 있었다.

1. Introduction

Epitaxial layers of InP have become increasingly important, due primarily to their suitability in optoelectronic and microwave device applications. For devices such as MIS transistors, FETs, solar cells, *p-i-n* photodiodes and avalanche photodiodes, a high purity epitaxial layer of InP is a fundamental requirement. The hydride VPE process has been an important growth technique for the InP related materials with certain advantages for large-scale production including high growth rate and process controllability. A limitation of hydride VPE, however, is imposed by the relatively high level of background doping (typically on the order of 5×10^{15} cm^{-3}, n-type), although lower values in the range 3×10^{14} - 6×10^{14} cm^{-3} have been reported [1]. This compares with the other growth techniques such as the liquid phase epitaxy (LPE) and the chloride VPE in which the background electron concentrations of less than 10^{15} cm^{-3} are routinely obtained [2,3]. Control of the background doping in the deposited film is a prerequisite for production of quality devices.

The background impurities incorporated into the epitaxial layers during growth have different origins. Impurities contained in the source materials used in the hydride VPE process such as the source gases (HCl, PH_3, H_2), the source metal (In), and the substrate (InP) can be the sources of background impurities. The chemicals used in the substrate preparation can be another source of impurities. Skromme et al. [4] identified some of the unintentional donors and acceptors in InP prepared by the hydride VPE, and they found Zn, C or Mg, and unidentifiable acceptor as background acceptors along with Si and S as background donors. Usui and Watanabe [5] analyzed the used indium by mass spectroscopy and detected a few ppm impurity contamination of Sn, Fe, and Cu which were hardly detected in the raw indium before the growth experiment. Their results showed that the In source has a gettering effect for inpurities in the input gases, mainly the HCl from a high pressure gas cylinder.

The use of a hot quartz wall (> 800℃) is another potential source of the background impurities in the hydride and chloride VPE processes. The interaction between the hot quartz (SiO_2) wall and the reactant gases may introduce Si as a background impurity. DiLorenzo and Moore [6] first proposed a thermodynamic model for the generation of vapor phase chlorosilanes as a result of the interaction of HCl with the quartz reactor wall and presented an expression for the activity of solid silicon (*i.e.*, as an impurity) as a function of the partial pressures of the chlorosilanes. This model showed that increasing the vapor HCl concentraction decreased the condensed phase silicon activity by further stabilizing the silicon species in the vapor phase in the form of chlorosilanes. Many experimental and thermodynamic studies [7-15] confirmed this model, especially in the growth of GaAs [7-10] and InP [11,12] by chloride VPE and in the growth of GaAs [13-15] by hydride VPE.

Some of the recent experimental studies of hydride VPE, however, are somewhat intriguing. Buckley [16] studied hydride VPE of $Ga_xIn_{1-x}As$ and found that the AsH_3, not the HCl, is the main factor determining the level of unintentional doping of the grown layers under conditions of constant growth rate. An inverse proportionality between carrier concentration and growth rate was observed, and a model was developed to account for this relationship which further supported his conclusion of AsH_3 being the main source of the unintentional dopant. Anderson [17] studied the growth of InP by hydride VPE in order to determine the effect of HCl mole fraction, H_2 flow rate, and mixing zone temperature on unintentional impurity incorporation. These parameters were found to produce only minor changes in the electrical behavior of the InP epitaxial layers.

The unintentional doping of the epitaxial InP grown by the hydride VPE technique is revisited in the present study. The effects of inlet mole fraction of HCl(x^0_{HCl}), inlet mole fraction of PH_3($x^0_{PH_3}$), and source zone temperature (T_s) on the extent of impurity incorporation were investigated in order to understand the chemistry involved in the background doping process. The variable temperature Hall effect system was used to measure the net carrier concentration and mobility of InP films, and the results are interpreted with respect to the process variables. In addition, an attempt was made to identify the major background impurities in the InP films. Low temperature (4.2 K) Fourier transform photoluminescence (FTPL) spectroscopy was employed for this purpose and the results are reported.

2. Experimental

The hydride VPE reactor used in this study had the conventional double-barrel reactor design and is schematically shown in Fig. 1. The reactor was successfully operated to grow device-quality InP epitaxial layers with mirror-like surface, and the typical operating conditions used were as follows : The source zone, the mixing zone, and the deposition zone were kept at 838℃, 820℃, and 700℃, respectively. The reactor pressure was at 1 atm. The III/V ratio was fixed at one (20 sccm of HCl and 200 sccm of 10 % PH_3 in H_2), and the total volumetric flow rate was held constant at 4200 sccm (25 cm/s linear velocity). These typical operating conditions were used as the base operating conditions of this study, and the process variables such as the inlet mole fractions of HCl and PH_3 and the source zone temperature were then changed about these base operating conditions.

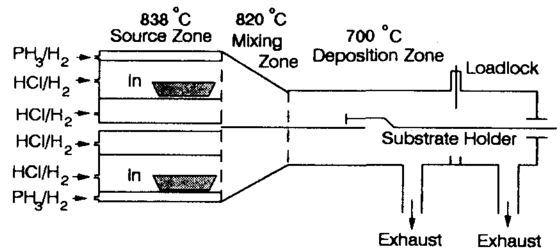

Fig. 1. Schematic of the hydride VPE double barrel reactor.

Phosphine was supplied as a 10 % mixture in hydrogen (Airco, VLSI grade), and the carrier hydrogen was purified by Pd-alloy diffusion. HCl (Airco, ULSI grade) was 99.999 % pure, and indium (RASA industries) was 99.99999 % pure. Substrates grown by the LEC method were Fe-doped InP (Crystacomm), cut 2° off the (100) toward the nearest (110).

The substrates were etched in Caro's acid (5 : 1 : 1 H_2SO_4 : H_2O_2 : H_2O) for 3 min. and in 1 % Br_2/CH_3OH solution for 2 min. just before loading. The etched substrate, typically about 1×1 cm^2, was placed into the reactor load-lock chamber and flushed with H_2 prior to opening the gate valve. Reactant flows were initiated about 15 min. prior to the insertion of substrates, and the substrate was preheated in a PH_3/H_2 mixture ($P^0_{PH_3}$= 3.9×10^{-2} atm) prior to deposition.

The thickness of InP epitaxial layers was measured by optical microscopy on cleaved and stained samples. Samples were stained by the solution of KOH (6 g) : $K_3Fe(CN)_6$ (4 g) in DI-water (50 cc). The background carrier concentration and mobility were measured by a variable temperature Hall effect system. The system was a custom design and its essential parts included a cryostage equipped with a resistive heater with temperature controller for temperature varying measurements, a magnet with constant current supply, and an electrometer. Measurements were made with magnetic flux density of 4600 gauss.

The background impurities were investigted by a Fourier transform photoluminescence (FTPL) spectroscopy [18,19]. The luminescence was excited by an argon ion laser of wavelength at 514.5 nm, and the power density at the sample was typically 0.18 W/cm^2 with an unfocused spot diameter of approximately 2 mm. Samples were placed in a bottom looking liquid helium immersion dewar and analysed in a backscattering configuration using f/1.2 collection optics. The measurement temperature was at 4.2 K. The interferometer employed for spectral analysis was the Twyman-Green version of the Michelson, that is, light from the source is collimated before being amplitude divided by the CaF_2 beamsplitter. A liquid nitrogen cooled Ge photovoltaic detector was employed as a detector. Interferograms were Fourier transformed using a cosine apodization function, and spectra were signal averaged 30 times. Energy calibration was made referenced to the HeNe vacuum wavenumber of 15798 cm^{-1}, and a spectral resolution of 2 cm^{-1} (0.25 meV) was used.

3. Results and discussion

Epitaxial layers of InP were grown for fixed deposition time of 10 min. with various process conditions. The initial characterization results of the grown layers and the corresponding process conditions are listed in Table 1. In general, the growth rate was found to increase with increasing x^0_{HCl}, indicating that the operating conditions used in this study are in the region where the HCl

Table 1
List of the process conditions and the preliminary charaterization results of undoped InP epitaxial layers

Sample No.	Source Temp.(℃)	X^{o}_{HCl} ($\times 10^3$)	$X^{o}_{PH_3}$ ($\times 10^3$)	III/V ratio	Layer Thick.(μm)	*FWHM (meV)
# 2723	770	4.739	4.739	1/1	7.4	29.6
# 2724	803	4.739	4.739	1/1	6.8	30.5
# 2725	838	4.739	4.739	1/1	6.8	30.1
# 2715	838	4.739	4.739	1/1	6.8	28.6
# 2729	887	4.739	4.739	1/1	6.3	34.5
# 2721	838	2.593	8.858	1/3	5.4	29.1
# 2720	838	4.525	9.050	1/2	6.3	31.7
# 2719	838	4.630	6.944	2/3	7.8	28.8
# 2716	838	7.092	4.728	3/2	8.5	30.2
# 2717	838	9.434	4.717	2/1	9.3	30.5
# 2718	838	14.085	4.695	3/1	12.9	32.2

* Values were taken from the room temperature (293 K) PL peaks at 1.34 eV.

conversion in the source zone is far from completion. Previous studies with the identical reactor showed that there is a maximum in growth rate typically around the III/V ratio of one [20]. The growth rate, however, was relatively independent of the inlet mole fraction of PH_3 ($x^0_{PH_3}$) and the source zone temperature (T_s). All the grown layers were analyzed by FTPL spectroscopy at room temperature (293 K), and the values of the full width at half maximum (FWHM) of the PL peaks at 1.34 eV are also listed in Table 1. No apparent trend of FWHM values was noticed with the change in the process variables, except for the sample #2729 (growth with the highest source zone temperature), which indicated that the crystallinity of the epitaxial layers was rather unaffected by the process variables changed in this study. Samples grown with extreme values of each process variable were thus selected for further characterization, and the results are discussed in the following paragraphs.

3.1. Hall measurement

The Hall data of the selected samples were obtained in the temperature range 35 to 300 K. Each InP sample was n-type. Samples grown with different source zone temperatures were first compared, and the results are shown in Figs. 2 and 3. Source zone temperature was varied at 770 ℃, 838℃, and 887℃, while the inlet mole fractions of HCl and PH_3 were kept constant at 4.739×10^{-3}. Two samples were grown with

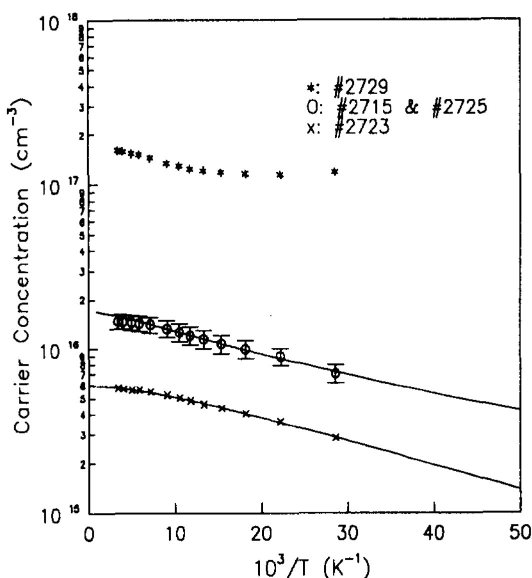

Fig. 2. Temperature dependent Hall data of VPE InP layers : carrier concentration is plotted against 1/T. Solid curves represent the theoretical data fit described in the text. Process conditions : *, T_s=887℃ ; O, T_s=838℃ ; ×, T_s=770℃ at $x^0_{PH_3}=4.739\times10^{-3}$ and $x^o_{HCl}=4.739\times10^{-3}$.

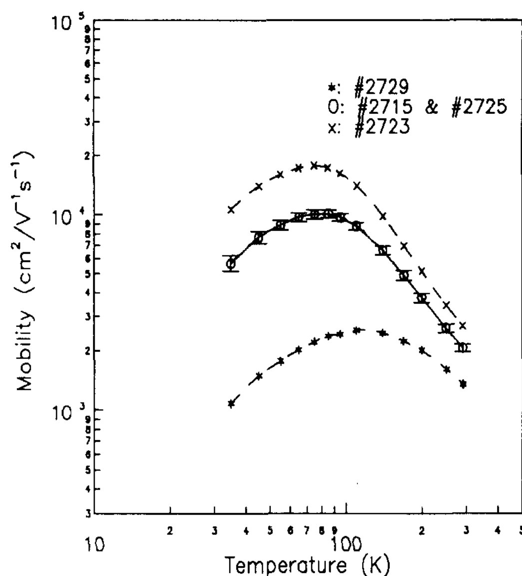

Fig. 3. Temperature dependent Hall data of VPE InP layers : mobility is plotted against T. Dashed curves merely connect the experimental data points. Process conditions : *, T_s =887℃ ; O, T_s=838℃ ; ×, T_s=770℃ at $x^0_{PH_3}=4.739\times10^{-3}$ and $x^0_{HCl}=4.739\times10^{-3}$.

source zone temperature of 838℃, thus the data are represented with error bars. As clearly shown in the figures, the background carrier concentration (Fig. 2) of the InP film increases and the mobility (Fig. 3) decreases dramatically, as the source zone temperature was raised. These results are consistent with an experimental observation by McCollum et al. [1]. A thermodynamic analysis [21] also predicts an increase in the background doping with increasing source zone temperature, since the formation of vapor phase silicon species increases with the increasing source zone temperature. Impurity gettering by the In source [5], however, was not observed in the present study.

The effect of varying the inlet mole fractions of HCl and PH_3 on the extent of impurity incorporation is shown in Fig. 4 (carrier concentration) and Fig. 5 (mobility). The background carrier concentration decreases and the mobility increases with the increase of inlet mole fraction of HCl. This result agrees with many experimental and thermodynamic studies [7-15] in the sense of DiLorenzo and Moore's model [6] in which the increased HCl lowers the background Si

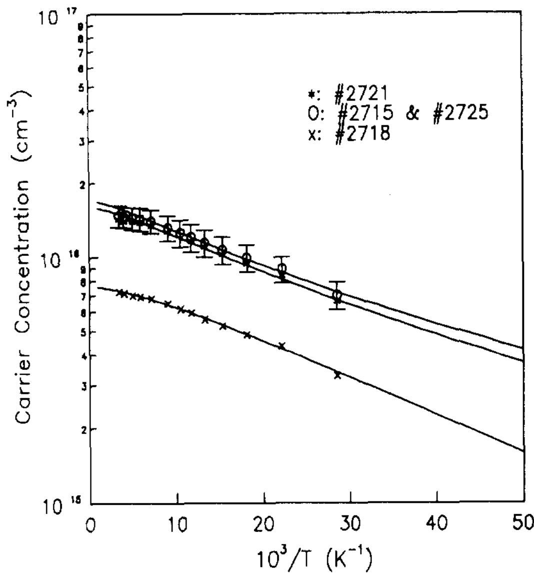

Fig. 4. Temperature dependent Hall data of VPE InP layers : carrier concentration is plotted against 1/T. Solid curves represent the theoretical data fit described in the text. Process conditions : O, $x^0_{PH_3}=4.739\times10^{-3}$ and $x^0_{HCl}=4.739\times10^{-3}$; *, $x^0_{PH_3}=8.858\times10^{-3}$ and $x^0_{HCl}=2.953\times10^{-3}$; ×, $x^0_{PH_3}=4.695\times10^{-3}$ and $x^0_{HCl}=14.085\times10^{-3}$ at $T_s=838℃$.

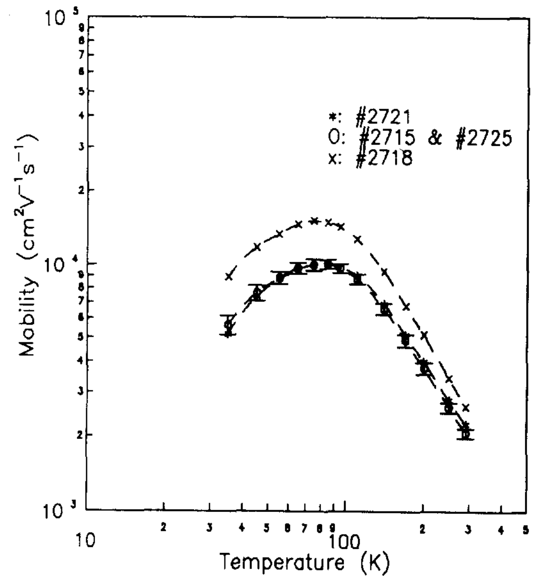

Fig. 5. Temperature dependent Hall data of VPE InP layers : mobility is plotted against T. Dashed curves merely connect the experimental data point. Process conditions : O, $x^0_{PH_3}=4.739\times10^{-3}$ and $x^0_{HCl}=4.739\times10^{-3}$; *, $x^0_{PH_3}=8.858\times10^{-3}$ and $x^0_{HCl}=2.953\times10^{-3}$; ×, $x^0_{PH_3}=4.695\times10^{-3}$ and $x^0_{HCl}=14.085\times10^{-3}$ at $T_s=838℃$.

doping of the film by stabilizing the silicon species in the vapor phase in the form of chlorosilanes. The dramatic decrease in the background doping with lowered source zone temperatures (Fig. 2) can also be understood in the same context that the reduced HCl conversion at lower source zone temperatures provides more HCl in the vapor phase. On the other hand, the background doping in the InP film seems not much affected by the change in the inlet mole fraction of PH_3, although a thermodynamic study [21] predicts the decrease in Si incorporation with increasing $x^0_{PH_3}$. A slight decrease of background carrier concentration was observed with increasing $x^0_{PH_3}$ (Fig. 4), but the magnitude of the change was within the error bar.

A simple theoretical analysis was performed to extract the electrical parameters of the InP films such as the electron concentration in the exhaustion region (N_d-N_a), the compensation ratio ($K=N_a/N_d$), and the ionization energy of donor level (E_d), where N_d is the donor level density and N_a is the acceptor level density. An analytical formu-

la [22] was used to fit the temperature dependence of electron concentration (n) Figs. 2 and 4).

$$n(T) = 2(N_d - N_a)\left(\left[1+\frac{N_a}{gN_c}\exp\left(\frac{E_d}{k_BT}\right)\right] + \left\{\left[1+\frac{N_a}{gN_c}\exp\left(\frac{E_d}{k_BT}\right)\right]^2 + \frac{4}{gN_c}(N_d - N_a)\exp\left(\frac{E_d}{k_BT}\right)\right\}^{0.5}\right)^{-1} \quad (1)$$

where g is the spin degeneracy factor which is equal to unity in the bands and 0.5 for donor levels. k_B is the Boltzmann constant.

The effective density of states for conduction bands (N_c) is given by,

$$N_c = 2\,(2\,\pi m_e K_B T/h^2)^{3/2} \quad (2)$$

where m_e is the electron band edge effective mass (m_e = 0.08 m_o is used in the calculation [22], where m_o is the free electron mass). h is the Planck's constant.

There are three unknowns in equation (1), which are ($N_d - N_a$), K, and E_d. Using the experimental data, one can easily estimate the parameters E_d and ($N_d - N_a$) in the first step. E_d can be estimated from low-temperature slope and ($N_d - N_a$) from electron concentration (n) in the exhaustion region extrapolating to high temperatures as 1/T approaches 0. The fitting procedure is then initiated with these estimated values of E_d and ($N_d - N_a$) obtained in the first step. The fit is best done by eye using trial and error method, systematically changing the values of the parameters until satisfactory agreement is achieved. The parameters obtained by this procedure are given in Table 2.

The equation (1) works well when ($N_d - N_a$) $< 3\times10^{16}$ cm^{-3}, and this condition was fulfilled for all InP samples characterized in this study except the sample #2729. Very good fits were obtained between the experimental data and the theoretical analysis over broad temperature range (see Figs. 2 and 4). The donor ionization energies of the InP samples were turned out to be generally

Table 2
Electrical parameters of undoped InP epitaxial layers

Sample No.	n at 77 K (cm^{-3})	μ at 77 K ($cm^2V^{-1}s^{-1}$)	$N_d - N_a$ (cm^{-3})	E_d (meV)	K
#2723	4.584×10^{15}	17788.8	6.0×10^{15}	2.4	0.31
*#2715	1.146×10^{16}	10020.2	1.7×10^{16}	1.5	0.11
*#2725	1.146×10^{16}	10020.2	1.7×10^{16}	1.5	0.11
#2729	1.211×10^{17}	2214.6	1.8×10^{17}	N/A	N/A
#2721	1.101×10^{16}	10068.8	1.6×10^{16}	2.0	0.08
#2718	5.574×10^{15}	15228.1	7.6×10^{15}	2.6	0.25

* Average values are listed for samples #2715 and #2725.

low compared to the values of higher purity InP films grown by the chloride VPE [22], and this was due to the fact that E_d depends on the concentration of impurities. It was shown that [22]

$$E_d = 7.4\,[1 - 3.9R_0(N_d - N_a)^{1/3}] \quad (3)$$

with

$$R_o = (m_o/m_e)\,\varepsilon a_o \quad (4)$$

where a_o is the Bohr radius and ε (=12.2) is the low frequency dielectric constant of InP. The equation (3) intercepts the vertical axis at the donor ionization energy obtained optically [23], and the linear extrapolation goes to zero at $N_d - N_a = 3.4\times10^{16}$ cm^{-3}. As a self-consistency check on the validity of the analysis, the values of E_d obtained from the fitting to the Hall data are plotted against $(N_d - N_a)^{1/3}$ in Fig. 6 and compared with the theoretical line given by the equation (3). It shows a reasonably good agreement, indicating that the procedure of extracting the electrical parameters is self-consistent. The small ionization energies of donor level can be explained by the relatively high background carrier concentration of the samples in this study ($7\times10^{15} - 2\times10^{17}$).

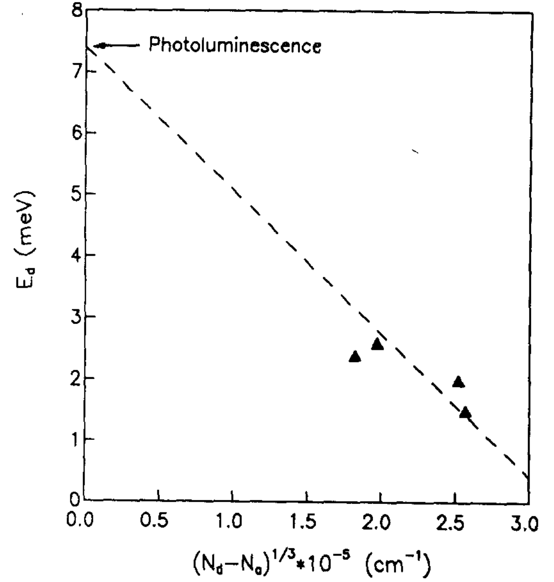

Fig. 6. Effective donor ionization energy deduced from fits to InP Hall data plotted against $(N_d - N_a)^{1/3}$. In the limit of no ionized impurities, E_d approaches the value obtained optically.

3.2. *FTPL measurement*

Fourier transform photoluminescence (FTPL) spectra were obtained at 4.2 K for all the InP samples listed in Table 1. Four bands, peaking at around 1.416, 1.401, 1.389 and 1.380 eV were easily identifiable for most of the samples (shown in Fig. 7 (a)), and another very broad and low intensity rise centered near 1.355 eV was also observed in all samples. The relative intensities of these bands were changed from sample to sample. To get more information about the correlation between the luminescence spectrum and the background impurities and to obtain more accurate parameters of the luminescence peaks, all the spectra were decomposed into elementary peaks by using a commercial Spectra Calc curvefit software (Galactic Industries). It was assumed that there are four elementary peaks in the entire spectrum which have Lorentzian shape

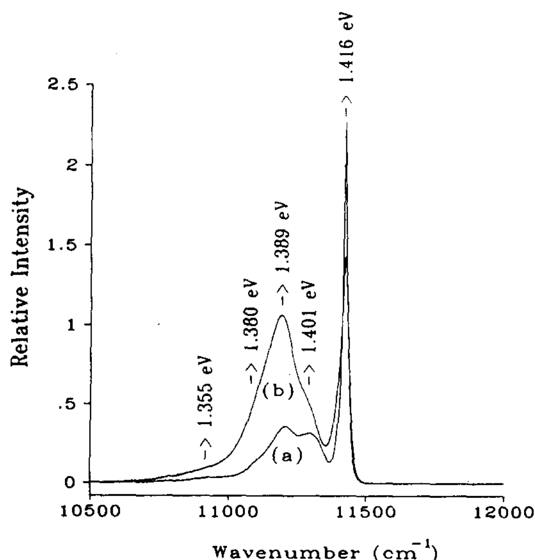

Fig. 7. FTPL spectra of sample (a) #2723 (T_s=770℃) and (b) #2729 (T_s=887℃). Other growth conditions are given in Table 1.

and are fully characterized by their three first momenta, *i.e.*, position of the peak, area under the peak, and full width at half maximum (FWHM) of the peak. No other restrictions were made for the curvefit. The curvefit was very good for all the spectra, and the parameters obtained by this procedure are listed in Table 3. The position of the elementary peaks did not change significantly among different samples, even though the entire spectrum changed its shape as a function of the process variables of this study. The change in the shape of spectra was caused mostly by the change in the area of the elementary peaks. The area under a peak is proportional to the concentration of the luminescence centers, and therefore it is closely related to the background impurity concentration.

Figure 7 shows two different FTPL spectra of the samples grown with different source zone temperatures. The increase of source zone temperature caused a remarkable change in the spectrum, and this was primarily due to the increased area of peak #3 at 1.389 eV and peak #4 at 1.380 eV (see Table 3). This is also consistent with the high background carrier concentration obtained in the sample #2729 (see Table 2 and Fig. 2). The area of peak #1 at 1.416 eV and peak #2 at 1.401 eV did not change significantly in these two samples. Figure 8 compares the two FTPL spectra of InP samples grown with different inlet mole fractions of HCl. The area of peak #3 and peak #4 decreased with increasing x^o_{HCl}, and this was again consistent with the lower carrier concentration of the sample #2718 (see

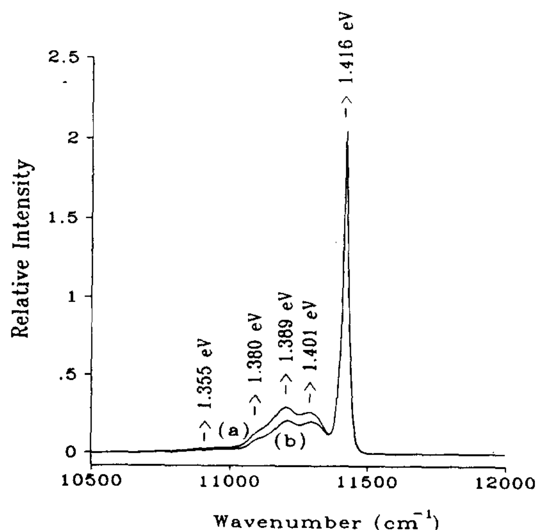

Fig. 8. FTPL spectra of sample (a) #2725 ($x^o_{HCl}=4.739\times10^{-3}$) and (b) #2718 ($x^o_{HCl}=14.085\times10^{-3}$). Other growth conditions are given in Table 1.

Table 3
Parameters of elementary peaks in the FTPL spectra of undoped InP epitaxial layers

Sample No.	Peak #1			Peak #2			Peak #3			Peak #4		
	Pos. (eV)	FWHM (meV)	Area	Pos. (eV)	FWHM (meV)	Area	Pos. (eV)	FWHM (meV)	Area	Pos. (eV)	FWHM (meV)	Area
#2723	1.416	2.33	60.9	1.401	9.91	28.0	1.390	12.91	41.2	1.381	17.29	21.9
#2715	1.416	2.76	99.6	1.401	9.67	25.7	1.389	12.76	35.6	1.378	13.08	15.7
#2725	1.416	2.95	70.5	1.401	9.05	21.0	1.389	12.58	34.7	1.380	15.92	18.6
#2729	1.416	3.87	64.9	1.399	10.20	29.7	1.388	12.87	118.1	1.380	18.54	97.5
#2721	1.416	2.79	74.8	1.401	9.22	29.7	1.389	12.74	53.8	1.380	15.74	26.7
#2718	1.416	2.76	66.6	1.401	10.63	19.4	1.389	12.45	24.5	1.379	15.21	10.1

Table 2 and Fig. 4). However, no apparent change in the FTPL spectra was observed when the inlet mole fraction of PH_3 was varied.

The FTPL spectra obtained in this study were carefully compared with the published PL spectra of InP films grown by various techniques such as the LEC [24,25], the LPE [26,27], the hydride VPE [1,26,28,29], the chloride VPE [30-33], the OMVPE [19, 29,34-37,40], and the MBE [38,39]. The elementary peaks obtained in this study were found to be much broader than the specific impurity related peaks found in the literature. The purest samples ($n < 10^{14}$ cm^{-3}) reported in the literature [1,35] show many very narrow peaks. The relatively large width of the peaks in this study was partially due to the relatively high level of background doping shown by the electrical measurements. At high carrier concentration ($> 3\times10^{16}$ cm^{-3}), the donor levels form a band. Most samples grown in this study had relatively high carrier concentration close to 1×10^{16} cm^{-3}, and thus the interaction between impurity centers are expected. This fact complicates the assignment of the peaks because usually it is possible to find several peaks in the literature whose frequencies fall in the region of one broad peak of this study. The high optical excitation used in this study could also shift the positon of the PL peaks. Acceptor related peaks, for example, are known to shift to higher energy when excitation level is increased [35].

The assignment of the five bands observed in this study was tentatively made by comparision with the published PL spectra : (a) peak #1 at 1.416 eV - exciton bound to impurity level transitions (D^o-X, D^+-X, A^o-X, etc.) [1,25,28,30,37,38,40]; (b) peak #2 at 1.401 eV - exciton bound to deep level acceptor transitions or transitions due to deep donors (shallow donor-vacancy complexes or shallow donor interstitials) [25,27,37] ; (c) peak #3 at 1.389 eV - free

electron to acceptor transitions (e - A°) due to Si or unidentified acceptors [25,28,35] ; (d) peak #4 at 1.380 eV - Zn or unidentified acceptor related transitions (e - A°, D° - A°, etc.) [26,28 - 30,35,36] ; (e) broad band centered at 1.355 eV - phonon replicas [25, 28,37]. Peak #1 and #2 are thought to be related to tight excitons because their energies are lower than the typical values. The free exciton (X) transitions are embeded in the high frequency shoulder of peak #1 due to the relatively high impurity concentration. The peak #3 is strongly dependent on the source zone temperature, and Si from the quartz tube is a highly probable source of background doping. Zn, which is proposed to be primarily responsible for peak #4, may come from In metal where it is present as an impurity. Other unidentified acceptors seem to be present as background impurities, but the identification of these acceptors could not be done, since the FTPL spectra obtained in this study was not very well resolved.

4. Summary

Background impurities in the epitaxial layers of InP grown by the hydride VPE technique were investigated to understand the chemistry involved in the background doping process. The effects of source zone temperature and inlet mole fractions of HCl and PH_3 on the impurity incorporation were investigated by a variable temperature Hall measurement and a low temperature (4.2 K) Fourier transform photoluminescence spectroscopy. The background carrier concentration was found to decrease with decreasing source zone temperature and increasing HCl, but it was relatively independent of PH_3 for the range of mole fraction studied. The electrical parameters of the InP films were extracted from the temperature-dependent Hall data by using simple theoretical equations. Background impurities were identified by analyzing the FTPL spectra of the InP films. It was found that Si donors and Zn acceptors as well as some unidentified acceptors are the major impurities in the hydride VPE grown InP films. The observed behavior of unintentional doping in the InP films generally followed the thermodynamic predictions and the DiLorenzo and Moore's Si incorporation model.

Acknowledgement

This research was supported in part by the Yeungnam University Research Grants in 1995.

References

[1] M.J. McCollum, M.H. Kim, S.S. Bose, B. Lee and G.E. Stillman, Appl. Phys. Lett. 53 (1988) 1868.

[2] R.D. Fairman, M. Omori and F.B. Fank, Proc. 6th Intern. Symp. on Gallium Arsenide and Related Compounds (1976) 45.

[3] E. Kuphal and A. Pocker, J. Cryst. Growth 58 (1982) 133.

[4] B.J. Skromme, T.S. Low, T.J. Roth, G. E. Stillman, J.K. Kennedy and J.K. Abrokwah, J. Electron. Mat. 12 (1983) 433.

[5] A. Usui and H. Watanabe, J. Electron. Mat. 12 (1983) 891.

[6] J.V. DiLorenzo, G.E. Moore, Jr., J. Electrochem. Soc. 118 (1971) 1823.

[7] P. Rai-Choundhury, J. Cryst. Growth 11 (1971) 113.

[8] C.M. Wolfe, G.E. Stillman and D.M. Korn, Inst. Phys. Conf. Ser. 33b (1977) 127.

[9] L. Palm, H. Bruch, K. Bachem and D. J. Balk., J. Electron. Mat. 8 (1979) 555.

[10] H. Seki, A. Koukito, H. Seki and M. Fujimoto, J. Cryst. Growth 43 (1978) 159.

[11] R.C. Clarke, J. Cryst. Growth 23 (1974) 166.

[12] J. Chevrier, A. Huber and N.T. Linh, J. Cryst. Growth 47 (1979) 267.

[13] H.B. Pogge and B.M. Kemlage, J. Cryst. Growth 31 (1975) 183.

[14] J.K. Kennedy, W.D. Potter and D.E. Davies, J. Cryst. Growth 24 (1974) 233.

[15] R.E. Enstrom and J. Appert, J. Electrochem. Soc. 129 (1982) 2566.

[16] D.N. Buckley, J. Electrochem. Soc. 137 (1990) 1219.

[17] T.J. Anderson, Research Report, USAF Rome Air Development Center, F49620-79-C-0038.

[18] W.M. Duncan, SPIE Vol. 822, Raman and Luminescence Spectroscopy in Technology (1987) 172.

[19] N.L. Rowell, SPIE Vol. 822, Raman and Luminescence Spectroscopy in Technology (1987) 161.

[20] C. Park, V.S. Ban, G.H. Olsen, T.J. Anderson and K.P. Quinlan, J. Electron. Mat. 21 (1992) 447.

[21] K.A. Jones. J. Cryst. Growth 60 (1982) 313.

[22] D.A. Anderson and N. Apsley, The Institute of Physics (1986) 187.

[23] M.S. Skolnick and P.J. Dean, J. Phys. C : Solid State Phys. 15 (1982) 5863.

[24] M. Erman, G. Gillardin, J. Le Bris, M. Renaud and E. Tomzig, J. Cryst. Growth 96 (1989) 469.

[25] T. Inoue, H. Shimakura, K. Kainosho, R. Hirano and O. Oda, J. Electrochem. Soc. 137 (1990) 1283.

[26] B.J. Skromme, G.E. Stillman, J.D. Oberstar and S.S. Chan, Appl. Phys. Lett. 44 (1984) 319.

[27] U. Heim, O. Röder, H.J. Queisser and M. Pilkuhn, J. Luminescence 1 (1970) 542.

[28] G.S. Pomrenke, J. Cryst. Growth 64 (1983) 158.

[29] S.S. Bose, I. Szafranek, M.H. Kim and G.E. Stillman, Apply. Phys. Lett. 56 (1990) 752.

[30] J. Chevrier, A. Huber and N.T. Linh, J. Appl. Phys. 51 (1980) 815.

[31] R.D. Fairman, M. Omori and F.B. Fank, Inst. Phys. Conf. Ser. No. 33b (1977) 45.

[32] J. Chevrier, E. Horache, L. Goldstein and N.T. Linh, J. Appl. Phys. 53 (1982) 3247.

[33] P.J. Dean, M.S. Skolnick and L.L Taylor, J. Appl. Phys. 55 (1984) 957.

[34] N.D. Gerrard, D.J. Nicholas, J.O. Williams and A.C. Jones, Chemtronics 3 (1988) 17.

[35] L.D. Zhu, K.T. Chan, D.K. Wagner and J.M. Ballantyne, J. Appl. Phys. 57 (1985) 5486.

[36] K. Uwai, S. Yamada and K. Takahei, J. Appl. Phys. 61 (1987) 1059.

[37] O. Aina, M. Mattingly, S. Steinhauser, R. Mariella, Jr. and A. Melas, J. Cryst. Growth 92 (1988) 215.

[38] S. Ovadia and A. Iliadis, SPIE Vol. 822, Raman and Luminescence Spectroscopy in Technology (1987) 40.

[39] H. Heinecke, B. Bauer, R. Höger and A. Miklis, J. Cryst. Growth 105 (1990) 143.

[40] Y. Fujiwara, S. Furuta, K. Makita, Y. Ito, Y. Nonogaki and Y. Takeda, J. Cryst. Growth 146 (1995) 544.